International Journal of Heat and Fluid Flow 30 (2009) 443–451

Contents lists available at ScienceDirect

International Journal of Heat and Fluid Flow

journal homepage: www.elsevier.com/locate/ijhff

Transport and deposition of colliding particles in turbulent channel flows

Leonid I. Zaichik [a,*], Vladimir M. Alipchenkov [b], Artur R. Avetissian [c]

[a] Nuclear Safety Institute of the Russian Academy of Sciences, B. Tulskaya 52, 115191 Moscow, Russian Federation
[b] Institute for High Temperatures of the Russian Academy of Sciences, Krasnokazarmennaya 17a, 111116 Moscow, Russian Federation
[c] All Russian Nuclear Power Engineering Research and Development Institute, Cosmonaut Volkov Str. 6a, 125171 Moscow, Russian Federation

ARTICLE INFO

Article history:
Received 15 September 2008
Received in revised form 9 February 2009
Accepted 14 February 2009
Available online 29 March 2009

Keywords:
Turbulent flow
Particles
Collisions
Deposition
Channel

ABSTRACT

The purpose of this paper is twofold: (i) to present statistical models that describe particle–turbulence interactions as well as particle–particle collisions and (ii) to gain a better understanding of the effect of inter-particle collisions on transport, deposition, and preferential concentration of heavy particles in turbulent channel flows. The models presented are based on a kinetic equation for the probability density function of the particle velocity distribution in anisotropic turbulent flow. The model predictions compare reasonable well with numerical simulations and properly reproduce the crucial trends of computations.

1. Introduction

Two-phase particle-laden flows are encountered in many natural and industrial situations, and almost without exception these flows are turbulent. The existing strategies of modeling turbulent two-phase flows can be subdivided into two groups depending on the Lagrangian tracking and Eulerian continuum approaches for handling the particulate phase. In the framework of the Lagrangian method, the particles are assumed to encounter randomly a series of turbulent eddies, and the macroscopic particle properties are determined solving stochastic equations along separate trajectories. As a consequence, even in dilute two-phase flows, such a method requires tracking a very large number of particle trajectories to achieve statistically invariant solution. As the size of particles decreases, the representative number of realizations should increase because of the increasing contribution of particle interactions with turbulent eddies of smaller and smaller scale. When the fraction of the particulate phase rises, the Lagrangian tracking approach also becomes more time-consuming due to the increased part of inter-particle collisions. Thus, this technique provides a very useful research tool of investigating particle-laden flows, but it can be too expensive for engineering calculations.

The Eulerian method deals with the particulate phase in much the same manner as with the carrier fluid phase. Therefore, the two-fluid modeling technique is computationally very efficient, as it allows us to use the governing equations of the same type for both phases. In addition, the description of fine particles does not cause great difficulties because the problem of the transport of particles with vanishing response times reduces to the turbulent diffusion of a passive impurity (Zaichik, 1999). Moreover, in the framework of the Eulerian approach, a consideration of inter-particle collisions is not nearly as time-consuming and complicated as it is in the framework of Lagrangian simulation. Overall, the Lagrangian tracking and Eulerian continuum modeling methods complement each other. Each method has its advantages and, consequently, its own field of application. The Lagrangiam method is more applicable for non-equilibrium flows (e.g., high-inertia particles, dilute dispersed media), while the Eulerian method is preferable for flows that are close to equilibrium (e.g., low-inertia particles, dense dispersed media).

In this paper, we present statistical models for predicting the transport, dispersion, and deposition of colliding particles in the framework of the Eulerian continuum approach. The models start from a kinetic equation for the probability density function (PDF) of the particle velocity distribution in anisotropic turbulent flow. Application of this approach provides modeling both the interaction of particles with fluid turbulent eddies and the inter-particle interaction due to collisions. The particle–turbulence interaction is modeled by a second-order operator of the Fokker–Planck type, while the particle–particle interaction is described by an integral operator of the Boltzmann type. The validity of the models is proved by comparing predictions with numerical simulations performed in vertical flat channel flows with and without particle deposition onto the channel wall.

* Corresponding author. Tel.: +7 495 955 2394; fax: +7 495 958 1151.
E-mail address: zaichik@ibrae.ac.ru (L.I. Zaichik).

0142-727X/$ - see front matter © 2009 Elsevier Inc. All rights reserved.
doi:10.1016/j.ijheatfluidflow.2009.02.013

Nomenclature

d_p	particle diameter
e	collision restitution coefficient
g_i	gravity acceleration
h	channel half-width
J_w	deposition flow rate, $V_{2w}\Phi_w$
j_+	deposition coefficient, $J_w/u_*\Phi_b$
k	turbulence kinetic energy, $\langle u_i' u_i' \rangle/2$
L	turbulence spatial macroscale
m	turbulence structure parameter, $T_E u'/L$
Re_p	particle Reynolds number, $d_p\lvert\mathbf{u}-\mathbf{v}\rvert/\nu$
Re_*	Reynolds number, hu_*/ν
Re_λ	Taylor-scale Reynolds number, $(15u'^4/\varepsilon\nu)^{1/2}$
St_E	Stokes number, τ_p/T_E
T_E	Eulerian integral timescale
T_L	Lagrangian integral timescale
$T_{Lp\ ij}$	eddy–particle interaction timescales
t	time
U_i	average fluid velocity
$U_{p\ i}$	average fluid velocity seen by particles
u_i	fluid velocity
u_*	wall friction velocity
u'^2	fluid velocity variance, $2k/3$
$\langle u_i' u_j' \rangle$	fluid kinetic stresses
V_i	average particle velocity
v_i	particle velocity
v'^2	particle velocity variance
$\langle v_i' v_j' \rangle$	particle kinetic stresses
y	wall-normal coordinate
y_+	dimensionless wall-normal coordinate, yu_*/ν
x_i	spatial coordinate

Greek letters

ε	turbulence dissipation rate
ν	fluid kinematic viscosity
ρ	fluid density
τ_k	Kolmogorov timescale, $(\nu/\varepsilon^{1/2})$
τ_p	particle response time, $\tau_{p0}(1+0.15Re_p^{0.687})^{-1}$
τ_{p0}	Stokes particle response time, $\rho_p d_p^2/18\rho\nu$
τ_+	particle inertia parameter, $\tau_{p0}u_*^2/\nu$
Φ	particle volume fraction
χ	rebound coefficient

Subscripts

p	particle
w	wall
1, 2, and 3	longitudinal, wall-normal, and spanwise directions
+	wall units

One of the most interesting phenomena caused by the interaction of particles with fluid turbulent eddies is the formation of regions with particle preferential concentration. This is due to the so-called turbophoresis force induced by fluctuating velocity gradients (Caporaloni et al., 1975; Reeks, 1983). Marchioli and Soldati (2002) showed the governing role of coherent turbulent structures in particle accumulation and analyzed segregation mechanisms in the near-wall boundary flows. The question of special interest is whether the effects of segregation, near-wall accumulation, and collisions on the transport and deposition of particles can be successfully reproduced using the proposed approach. This is the primary motivation for the present research.

This paper addresses fluid turbulent flows laden with small heavy identical particles. The particle size is assumed to be less than the Kolmogorov length scale and the particle mass fraction is assumed to be low in order for the back-effect of particles on the fluid turbulence to be negligible.

2. Mathematical formulation

The theoretical background of the models is a transport kinetic equation for the one-particle PDF, P_1, that is the probability of finding a particle at a point $\mathbf{x}$, with a velocity $\mathbf{v}$, at time t. This kinetic equation has the form

$$\frac{\partial P}{\partial t}+v_i\frac{\partial P}{\partial x_i}+\frac{\partial}{\partial v_i}\left[\left(\frac{U_i-v_i}{\tau_p}+g_i\right)P\right] = \lambda_{ij}\frac{\partial^2 P}{\partial v_i\partial v_j}+\mu_{ij}\frac{\partial^2 P}{\partial x_i\partial v_j}+\left(\frac{\partial P}{\partial t}\right)_{coll}. \quad (1)$$

The first two terms on the right-hand side of Eq. (1) describe the interaction of particles with fluid turbulent eddies, and the third term quantifies the contribution of inter-particle collisions. To determine the particle–turbulence interaction terms, we model the fluid turbulence by a Gaussian random process and use the functional formalism (Zaichik, 1999; Zaichik et al., 2004; Zaichik and Alipchenkov, 2005). The modeling of the fluid velocity field by the Gaussian process is the key assumption that allows us to present the particle–turbulence interaction in the form of a second-order differential operator. This operator is expressed in terms of the turbulent stresses and average velocity gradients of the carrier fluid (see Appendix A).

The collision operator is written in the form of the Boltzmann integral as applied to the hard-sphere collision scheme

$$\left(\frac{\partial P}{\partial t}\right)_{coll}=d_p^2\int\int_{\mathbf{w}\cdot\mathbf{k}<0}\left[P_2(\mathbf{x},\mathbf{v}^\circ,\mathbf{x}+d_p\mathbf{k},\mathbf{v}_1^\circ,t) -P_2(\mathbf{x},\mathbf{v},\mathbf{x}+d_p\mathbf{k},\mathbf{v}_1,t)\right](\mathbf{w}\cdot\mathbf{k})d\mathbf{k}d\mathbf{v}_1, \quad (2)$$

where $\mathbf{w}\equiv\mathbf{v}_1-\mathbf{v}$ is the relative velocity of colliding particles, $\mathbf{k}$ is the unit vector directed along the line that joins the centers of colliding particles, P_2 is the two-particle PDF, $\mathbf{v}^\circ$ and $\mathbf{v}_1^\circ$ are the velocities of two particles after a collision, and the condition $\mathbf{w}\cdot\mathbf{k}<0$ indicates that the integration is carried out over the values of $\mathbf{k}$ and $\mathbf{v}_1$ for which particle collisions can be realized.

The kinetic equation completely controls the velocity statistics of the particulate phase. However, for most practical applications, the kinetic level of modeling is not only computationally too expensive, but is also unnecessary because macroscopic properties are usually all that are needed. Another computationally less expensive way is to solve the conservation equations for several first moments of the PDF. The kinetic equation generates the following set of governing conservation equations for the volume fraction, the average velocity, the kinetic stresses, and the third fluctuating velocity moments of the particulate phase:

$$\frac{\partial\Phi}{\partial t}+\frac{\partial\Phi V_i}{\partial x_i}=0, \quad (3)$$

$$\frac{\partial V_i}{\partial t}+V_j\frac{\partial V_i}{\partial x_j}=-\frac{\partial\langle v_i'v_j'\rangle}{\partial x_j}+\frac{U_i-V_i}{\tau_p}+g_i-\frac{D_{p\ ij}}{\tau_p}\frac{\partial\ln\Phi}{\partial x_j},$$
$$D_{p\ ij}=\tau_p(\langle v_i'v_j'\rangle+\mu_{ij}), \quad (4)$$

$$\frac{\partial\langle v_i'v_j'\rangle}{\partial t}+V_k\frac{\partial\langle v_i'v_j'\rangle}{\partial x_k}+\frac{1}{\Phi}\frac{\partial\Phi\langle v_i'v_j'v_k'\rangle}{\partial x_k} =-(\langle v_i'v_k'\rangle+\mu_{ik})\frac{\partial V_j}{\partial x_k}-(\langle v_j'v_k'\rangle+\mu_{jk})\frac{\partial V_i}{\partial x_k}+\lambda_{ij}+\lambda_{ji}-\frac{2\langle v_i'v_j'\rangle}{\tau_p}+\mathbb{C}_{ij}, \quad (5)$$

$$\frac{\partial\langle v_i' v_j' v_k'\rangle}{\partial t}+V_n\frac{\partial\langle v_i' v_j' v_k'\rangle}{\partial x_n}$$
$$=-\langle v_i' v_j' v_n'\rangle\frac{\partial V_k}{\partial x_n}-\langle v_i' v_k' v_n'\rangle\frac{\partial V_j}{\partial x_n}-\langle v_j' v_k' v_n'\rangle\frac{\partial V_i}{\partial x_n}-(\langle v_i' v_n'\rangle+\mu_{in})$$
$$\times\frac{\partial\langle v_j' v_k'\rangle}{\partial x_n}-(\langle v_j' v_n'\rangle+\mu_{jn})\frac{\partial\langle v_j' v_k'\rangle}{\partial x_n}-(\langle v_k' v_n'\rangle+\mu_{kn})\frac{\partial\langle v_i' v_j'\rangle}{\partial x_n}$$
$$-\frac{3\langle v_i' v_j' v_k'\rangle}{\tau_p}+\mathbb{C}_{ijk}. \tag{6}$$

It is seen that collisions do not make a contribution to Eqs. (3) and (4) since they do not change the mass and the momentum of the particulate phase. However, collisions contribute to Eqs. (5) and (6), as represented by $\mathbb{C}_{ij}$ and $\mathbb{C}_{ijj}$. Eq. (6) is closed by means of representing the fourth-rank moments as a sum of the products of the second-order moments.

3. Modeling of collisions

For small volume fractions ($\Phi\leqslant 0.01$), the direct contribution of collisions to the stresses and the velocity fluctuation fluxes of the particle-phase can be neglected. This means that, in the moment-equations, the collision terms take the form of sources and do not contain flux-like components. Thus, the collision terms in (5) and (6) can be represented in the following form (Jenkins and Richman, 1985):

$$\mathbb{C}_{ij}=\frac{1}{\Phi}\int v_i' v_j'\left(\frac{\partial p}{\partial t}\right)_{coll}d\mathbf{v}$$
$$=\frac{6}{\pi d_p\Phi}\int_{w\cdot k<0}\int\int(\mathbf{w}\cdot\mathbf{k})P_2(\mathbf{x},\mathbf{v},\mathbf{x}+d_p\mathbf{k},\mathbf{v}_1,t)\{v_i' v_j'\}d\mathbf{k}d\mathbf{v}d\mathbf{v}_1, \tag{7}$$

$$\mathbb{C}_{ijk}=\frac{1}{\Phi}\int v_i' v_j' v_k'\left(\frac{\partial P}{\partial t}\right)_{coll}d\mathbf{v}$$
$$=\frac{6}{\pi d_p\Phi}\int_{\mathbf{w}\cdot\mathbf{k}<0}\int\int(\mathbf{w}\cdot\mathbf{k})P_2(\mathbf{x},\mathbf{v},\mathbf{x}+d_p\mathbf{k},d\mathbf{v}_1,t)\left\{v_i' v_j' v_k'\right\}d\mathbf{k}d\mathbf{v}d\mathbf{v}_1, \tag{8}$$

$$\{v_i' v_j'\}=\frac{1}{4}(1+e)(\mathbf{w}'\cdot\mathbf{k})[(1+e)(\mathbf{w}'\cdot\mathbf{k})k_i k_j-(w_i' k_j+w_i' k_j)],$$
$$\{v_i' v_j' v_k'\}=\frac{1}{4}(1+e)(\mathbf{w}'\cdot\mathbf{k})\Big[k_i(v_j' v_k'-v_{1j}' v_{1k}')$$
$$+k_j(v_i' v_k'-v_{1i}' v_{1k}')+k_k(v_i' v_j'-v_{1i}' v_{1j})\Big]$$
$$+\frac{(1+e)^2}{8}(\mathbf{w}'\cdot\mathbf{k})^2[k_i k_j(v_k'+v_{1k}')+k_i k_k(v_j'+v_{1j}')+k_j k_k(v_i'+v_{1i}')].$$

As follows from (7) and (8), in order to find the collision terms, it is necessary to determine the PDF of the velocities of two particles at the instant of collision. For this purpose, we use a statistical approach based on a Grad-like expansion of the two-particle velocity PDF. The first term of this expansion gives the Gaussian velocity distribution which is feasible for isotropic turbulence (Laviéville et al., 1995; Zaichik et al., 2003), whereas the second and third ones provide the contribution of velocity anisotropy to the particulate stresses and the triple moments. In accordance with the Grad method, the two-particle PDF is represented as an expansion in the Hermite polynomials. Note that, as is compared with other basis functions, the advantage of using the Hermite polynomials consists in the fact that the expansion coefficients can be expressed in terms of the PDF moments of the considered degree. Thus we represent the two-particle PDF as

$$P_2^{(1)}(\mathbf{v}_1,\mathbf{v}_2)=\left[1+\frac{(\langle v_i' v_j'\rangle-v'^2\delta_{ij})}{2!}\sum_{\alpha=1,2}\frac{\partial^2}{\partial v_{\alpha i}\partial v_{\alpha j}}\right.$$
$$+\frac{f_u(\langle v_i' v_j'\rangle-v'^2\delta_{ij})}{2!}\sum_{\substack{\alpha,\beta=1,2\\ \alpha\neq\beta}}\frac{\partial^2}{\partial v_{\alpha i}\partial v_{\beta j}}-\frac{\langle v_i' v_j' v_k'\rangle}{3!}$$
$$\left.\times\sum_{\alpha=1,2}\frac{\partial^3}{\partial v_{\alpha i}\partial v_{\alpha j}\partial v_{\alpha k}}-\frac{f_u\langle v_i' v_j' v_k'\rangle}{3!}\sum_{\substack{\alpha,\beta=1,2\\ \alpha\neq\beta}}\frac{\partial^3}{\partial v_{\alpha i}\partial v_{\alpha j}\partial v_{\beta k}}\right]P_2^{(0)}(\mathbf{v}_1,\mathbf{v}_2), \tag{9}$$

$$P_2^{(0)}(\mathbf{v},\mathbf{v}_1)=\frac{\Phi^2}{(2\pi v'^2)^3(1-f_u^2)^{3/2}}\exp\left(-\frac{v_k' v_k'+v_{1k}' v_{1k}'-2f_u v_k' v_{1k}'}{2v'^2(1-f_u^2)}\right),$$
$$f_u=\frac{1}{\tau_p}\int_0^\infty\Psi_{Lp}(\tau)\exp\left(-\frac{\tau}{\tau_p}\right)d\tau$$

with f_u being the coefficient that measures a response of particles to fluid turbulence, and $\Psi_{Lp}(\tau)$ being the autocorrelation function of the fluid fluctuating velocities seen by the particles. The particle response coefficient f_u decreases and tends to zero as τ_p increases, it means that the high-inertia particles move with velocities which are uncorrelated with each other and with the fluid flow.

Substituting (9) into (7) and (8) and performing integration, we obtain the following expressions for the second- and third-order collision terms:

$$\mathbb{C}_{ij}=-\frac{2(1-e^2)(1-f_u)k_p}{9\tau_c}\delta_{ij}-\frac{2(1-f_u)}{\tau_{c1}}\left(\langle v_i' v_j'\rangle-\frac{2}{3}k_p\delta_{ij}\right), \tag{10}$$

$$\mathbb{C}_{ijk}=-\frac{3(1-f_u)}{\tau_{c1}}\Big[\langle v_i' v_j' v_k'\rangle-E\big(\langle v_i' v_n' v_n'\rangle\delta_{jk}$$
$$+\langle v_j' v_n' v_n'\rangle\delta_{ik}+\langle v_k' v_n' v_n'\rangle\delta_{ij}\big)\Big], \tag{11}$$

$$\tau_c=\frac{d_p}{16\Phi(1-f_u)^{1/2}}\left(\frac{2\pi}{3k_p}\right)^{1/2},\quad \tau_{c1}=\frac{10\tau_c}{(1+e)(3-e)},\quad E=\frac{1+3e}{18(3-e)}.$$

Here, τ_c and τ_{c1} are the characteristic timescales of particle collisions, and $k_p\equiv\langle v_i' v_i'\rangle/2$ is the particle kinetic turbulent energy. The importance of particle–particle collisions relative to particle–turbulence interactions can be evaluated from the ratio of the particle response time to the collision timescale, τ_p/τ_c. For $\tau_p/\tau_c\ll 1$, the role of collisions is insignificant, while for $\tau_p/\tau_c\gg 1$ collisions play a decisive role in forming particle velocity statistics.

In accordance with (10), the effect of collisions on the particulate stresses is manifested in two ways: (i) the dissipation of particle velocity fluctuations due to inelastic collisions and (ii) the redistribution of the kinetic energy of particle velocity fluctuations between different components. The second effect is proportional to the rate of the anisotropy of particle velocity fluctuations and provides the tendency of $\langle v_i' v_j'\rangle$ towards an isotropic state. This is similar to the effect of pressure fluctuations on the fluid turbulent stresses (Rotta, 1951).

It should be noted that, in the case of elastic collisions ($e=1$), Laviéville et al. (1997) obtained a more general relation for the second-order collision term as compared to (10). The approach of Laviéville et al. (1997) relied on a Grad-like expansion for the joint fluid-particle PDF rather than for the two-particle PDF, and it provided the contribution not only the anisotropy of particle fluctuating velocities but the anisotropies of fluid velocity fluctuations and fluid-particle velocity covariances as well. However, this approach is too cumbersome for obtaining the third-order collision term. Although the second-order collision terms derived by two approaches are coincident only in the local-equilibrium approximation, the results obtained using both of these collision terms are quite close even in highly non-equilibrium anisotropic flows.

Within the framework of the Grad 13-moment approximation, the following relation between the triple correlations and their contractions takes place (Jenkins and Richman, 1985):

$$\langle v_i' v_j' v_k'\rangle=\frac{1}{5}\Big(\langle v_i' v_n' v_n'\rangle\delta_{jk}+\langle v_j' v_n' v_n'\rangle\delta_{ik}+\langle v_k' v_n' v_n'\rangle\delta_{ij}\Big). \tag{12}$$

Inserting (12) into (11) yields

$$\mathbb{C}_{ijk}=-\frac{3(1-f_u)}{\tau_{c2}}\langle v_i' v_j' v_k'\rangle,\quad \tau_{c2}=\frac{180\tau_c}{(1+e)(49-33e)}. \tag{13}$$

It is clear from (13) that the collisions result in a decrease in the triple correlations of particulate velocity fluctuations. As $f_u\to 0$, formulas (10), (11), and (13) are transformed into those obtained by

Jenkins and Richman (1985) for the collision terms in the case of non-correlated chaotic motion of particles. With decreasing particle inertia, the correlation of motion of two particles increases, this leads to an enhancement of the particle response coefficient f_u and a reduction in the effect of collisions on velocity statistics of the particulate phase.

If the terms describing the time evolution, the convection, and the third-moment generation due to average velocity gradients are neglected in (6) and Eq. (13) is taken into account, we can obtain the gradient algebraic relation for the third-order particle velocity fluctuations

$$\langle v_i' v_j' v_k' \rangle = -\frac{[1+(1-f_u)\tau_p/\tau_{c2}]^{-1}}{3} \times \left(D_{p\,in}\frac{\partial \langle v_j' v_k' \rangle}{\partial x_n} + D_{p\,jn}\frac{\partial \langle v_i' v_k' \rangle}{\partial x_n} + D_{p\,kn}\frac{\partial \langle v_i' v_j' \rangle}{\partial x_n} \right). \quad (14)$$

Eq. (14)) predicts a reduction in the influence of collisions on the diffusion transport of velocity fluctuations as the particle inertia decreases and thereby the correlation of particle velocities increases. When the correlation of particle velocities is absent ($f_u = 0$), Eq. (14) reduces to that obtained by Simonin (1991, 1996) for elastic and inelastic collisions.

Approximation (14) provides modeling the transport of the particulate phase at the second-moment level. In what follows, we use the second-moment model presented above to analyze the transport of particles in both the absence and the presence of deposition onto the channel wall.

4. Boundary conditions

To predict the particle transport and deposition we need knowledge of boundary conditions for governing equations. Relevant boundary conditions were derived solving the kinetic PDF equation in the near-wall region of the flow by means of perturbation techniques (Alipchenkov et al., 2001; Zaichik and Alipchenkov, 2001). The particle deposition rate obtained by this means is written as

$$V_{2w} = -\frac{1-\chi}{1+\chi}\left(\frac{2\langle v_2'^2 \rangle}{\pi}\right)^{1/2}_{y=0} \quad (15)$$

with χ being a probability of particle rebound from the wall and its return into the flow after collision. The surface is perfectly adsorbing if $\chi = 0$, and the particle deposition is absent if $\chi = 1$.The boundary conditions for the longitudinal $\langle v_1'^2 \rangle$, wall-normal $\langle v_2'^2 \rangle$, spanwise $\langle v_3'^2 \rangle$, and shear $\langle v_1' v_2' \rangle$ components of the particulate stresses on the wall (y = 0) have the following form:

$$\begin{aligned}
\tau_{p*}\frac{d\langle v_1'^2 \rangle}{dy} &= 3\left(\frac{1-\chi e_1^2}{1+\chi e_1^2} - \frac{1-\chi}{1+\chi}\right)\left(\frac{2}{\pi\langle v_2'^2 \rangle}\right)^{1/2}\langle v_1'^2 \rangle, \\
\tau_{p*}\frac{d\langle v_2'^2 \rangle}{dy} &= \left(2\frac{1-\chi e_2^2}{1+\chi e_2^2} - \frac{1-\chi}{1+\chi}\right)\left(\frac{2\langle v_2'^2 \rangle}{\pi}\right)^{1/2}, \\
\tau_{p*}\frac{d\langle v_3'^2 \rangle}{dy} &= 3\left(\frac{1-\chi e_3^2}{1+\chi e_3^2} - \frac{1-\chi}{1+\chi}\right)\left(\frac{2}{\pi\langle v_2'^2 \rangle}\right)^{1/2}\langle v_3'^2 \rangle, \\
\langle v_1' v_2' \rangle &= -\left(\frac{1-\chi e_1}{1+\chi e_1} - \frac{1-\chi}{1+\chi}\right)\left(\frac{2\langle v_2'^2 \rangle}{\pi}\right)^{1/2} V_{1w},
\end{aligned} \quad (16)$$

where $\tau_{p*} \equiv \tau_p \tau_{c2}/[\tau_p(1-f_u)+\tau_{c2}]$ denotes the effective particle response time, and V_{1w} designates the streamwise wall particle velocity. In (16), the restitution coefficients e_1, e_2, and e_3 measure the momentum loss during the bouncing process, respectively, in the longitudinal, wall-normal, and spanwise directions. The effect of inter-particle collisions on the boundary conditions manifests itself in virtue of the diffusion transport mechanism by substituting the effective response time τ_{p*} for the response time τ_p.

5. Particle transport in a vertical channel

First we examine the performance of the particle–turbulence interaction model for the transport of particles in a vertical flat channel flow without particle deposition when neglecting inter-particle collisions. In this case, the model incorporates the governing Eqs. (3)–(5) with $\mathbb{C}_{ij=0}$, the third-order approximation (14) with $\tau_{c2} = \infty$, and the boundary conditions (15) and (16) with $\chi = 1$. The flow is considered away from the channel inlet and is presumed to be fully developed. This means that the characteristics of the fluid and particulate phases are independent of the streamwise coordinate, x_1, and are only functions of the normal-wall coordinate, $x_2 = y$. The set of ordinary differential equations obtained by this means is solved numerically using the tridiagonal-matrix algorithm along with an iteration procedure.

In order to analyze the effect of particle inertia, we compare predictions with two sets of numerical simulations performed by Picciotto et al. (2005) for low-inertia particles and by Rouson and Eaton (1994), Wang and Squires (1996), and Fukagata et al. (1998) for high-inertia particles with no consideration of the feedback of particles on the fluid flow. In Picciotto et al. (2005), the gravity force was neglected and the Reynolds number, Re^*, was taken equal to 150. Simulations by Rouson and Eaton (1994), Wang and Squires (1996), and Fukagata et al. (1998) were carried out with the gravity force taken into account for the downward flow at $Re^* = 180$. In these works, the interaction of particles with the wall was assumed to be elastic. Consequently, when running comparisons with the simulations, the restitution coefficients in (16) were taken equal to unity. Here and hereafter the dimensionless variables were defined using wall units as follows: $U_{1+} = U_1/u_*$, $V_{1+} = V_1/u_*$, $u_{i+}' = \langle u_i'^2 \rangle^{1/2}/u_*$, $v_{i+}' = \langle v_i'^2 \rangle^{1/2}/u_*$, and $y_+ = y u_*/\nu$; the particle volume fraction was normalized with its value at the channel axis, $\overline{\Phi} = \Phi/\Phi(R)$.Fig. 1 demonstrates the distributions of average longitudinal velocity, all non-zero components of kinetic stresses, and particle concentration over the channel cross-section at relatively small values of inertia parameter τ_+. As is seen from Fig. 1a, the average velocity of particles, V_{1+}, slightly deviates from the fluid velocity, U_{1+}, even at $\tau_+ = 25$. According to Picciotto et al. (2005), the particle velocity slightly exceeds the fluid velocity in the region $1 < y_+ < 10$; the opposite is true for the region $10 < y_+ < 60$. In the near-wall region, the particle longitudinal fluctuating velocity exceeds the fluid one (Fig. 1b). As is seen, the maximum of v_{1+}' increases with τ_+, if not so markedly as this was suggested in the DNS. It should be noted that, as follows from Eq. (5), there are two mechanisms of generation of the longitudinal and shear components of particle kinetic stresses: (i) the generation of particle velocity fluctuations due to the gradient of average particle velocity and (ii) the generation resulting from the direct interaction of particles with fluid turbulent eddies (this is specified by λ_{ij}). The growth of v_{1+}' is explained by the gradient mechanism of the generation of fluctuations. The wall-normal and spanwise components of particle velocity fluctuations decrease with increasing particle inertia (Fig. 1c and d). One of the reasons for this is the absence of the gradient mechanism of the generation of the transverse components of particle velocity fluctuations; the other reason is a weaker response of particles to fluid velocity fluctuations as their inertia increases. When τ_+ grows, the magnitude of the shear stress component first rises over the channel cross-section due to the gradient generation mechanism and then falls because of decreasing the response of particles to fluid turbulence (Fig. 1e). It appears from Fig. 1e that the inertia of particles strongly alters their distribution over the channel cross-section. Relative to the case of zero-inertia particles we can observe that the concentration of inertial particles strongly rises in the viscous sub-layer adjacent to the wall, where the gradient of the wall-normal fluctu-

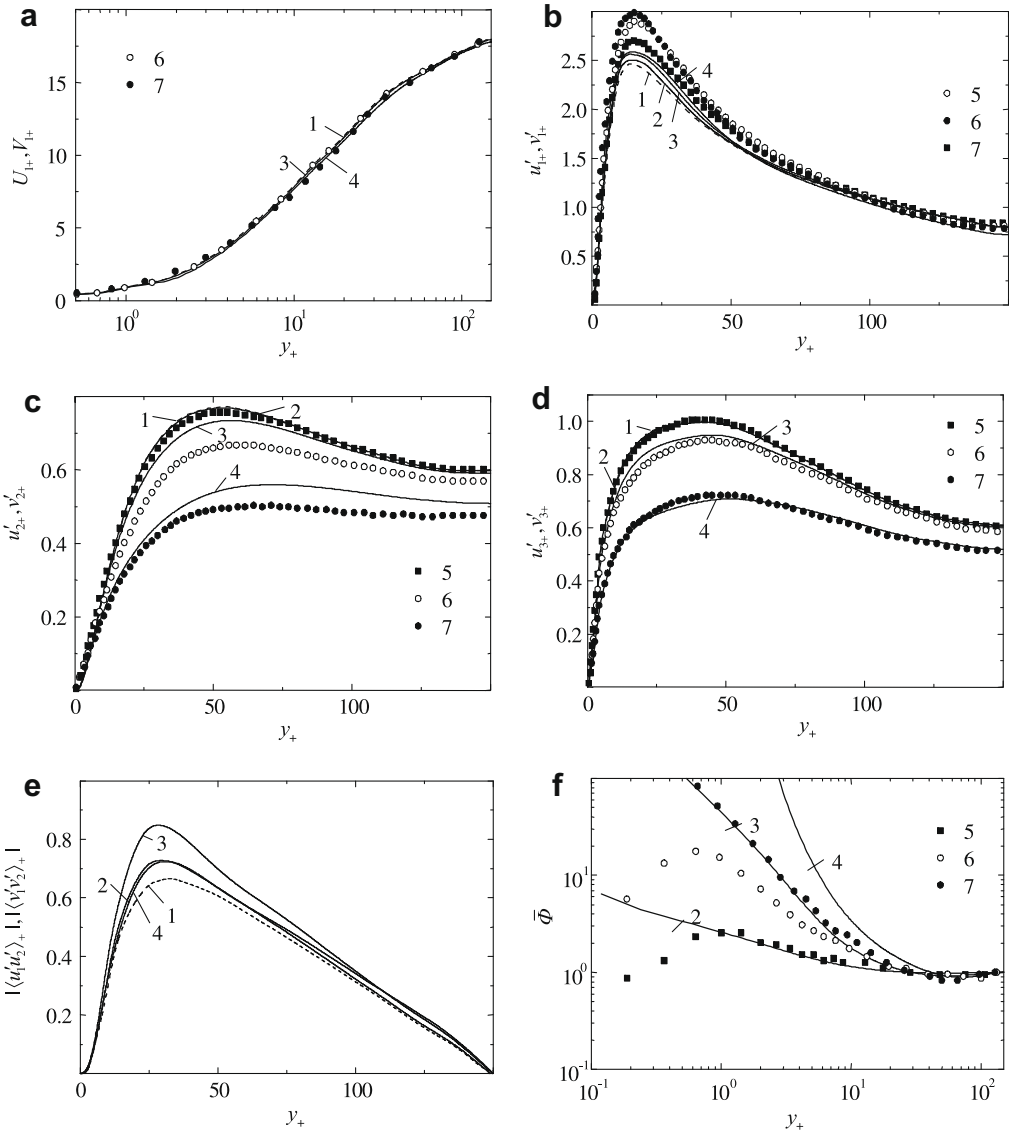

Fig. 1. Profiles of low-inertia particle characteristics over the channel cross-section: 1 – fluid; 2–7 – particles; 2–4 – predictions; 5–7 – DNS by Picciotto et al. (2005); 2, 5 – $\tau_+ = 1$; 3, 6 – $\tau_+ = 5$; 4, 7 – $\tau_+ = 25$.

ating velocity of the carrier fluid reaches its highest value. Some discrepancies between the predictions and the simulations are attributable to an error that is introduced by Eq. (14). This approximation of the triple particle fluctuating velocity correlations is more valid for higher particle inertia when the particle velocity distribution is nearly Gaussian.

Fig. 2 shows the distributions of particulate characteristics over the channel cross-section at large values of inertia parameter τ_+. The key feature of the average velocity profile is that it becomes flatter as particle inertia increases (Fig. 2a); this fact was pointed out in many experimental and numerical studies (e.g., see, Lee and Durst, 1982; Tsuji et al., 1984). As is clear from Fig. 2b, the maximum of the longitudinal fluctuating velocity component shifts towards the wall and the intensity of v'_{1+} at the wall increases with τ_+. For high-inertia particles ($\tau_+ = 810$), we observe a monotonous increase in v'_{1+} from the channel axis to the wall where v'_{1+} reaches its maximum value, even though the model predicts a somewhat smaller value of the maximum than that given by the numerical simulations. Fig. 2c and d shows that, due to the intensive diffusion transport of velocity fluctuations in the wall-normal direction, the profiles of v'_{2+} and v'_{3+} flatten and tend to homogeneous distributions with increasing τ_+. In the case of the elastic interaction of particles with the wall, the asymptotic distributions of the transverse velocity fluctuation components have the following form:

$$\lim_{\tau_p \to 0} \langle v_i'^2 \rangle = \frac{1}{\tau_p h} \int_0^h T_{Lp}^n \langle u_i'^2 \rangle dy, \quad i = 2, 3.$$

The shear stress falls off with τ_+ everywhere over the channel cross-section (Fig. 2e). This is explained, on the one hand, by a weaker influence of the gradient mechanism of the generation of velocity fluctuations due to the flattening of the average velocity profile and, on the other hand, by decreasing the response of particles to the turbulent motion of the fluid. Fig. 2f demonstrates a decrease in the concentration of high-inertia particles near the wall with τ_+. This is due to the flattening of the wall-normal fluctuating velocity profile and the resultant decrease in the turbophoresis driving force.

As one can observe from Figs. 1 and 2, the model describing the particle–turbulence interaction reproduces with some degree of certainty all of the effects found in the numerical simulations for both low-inertia and high-inertia particles.

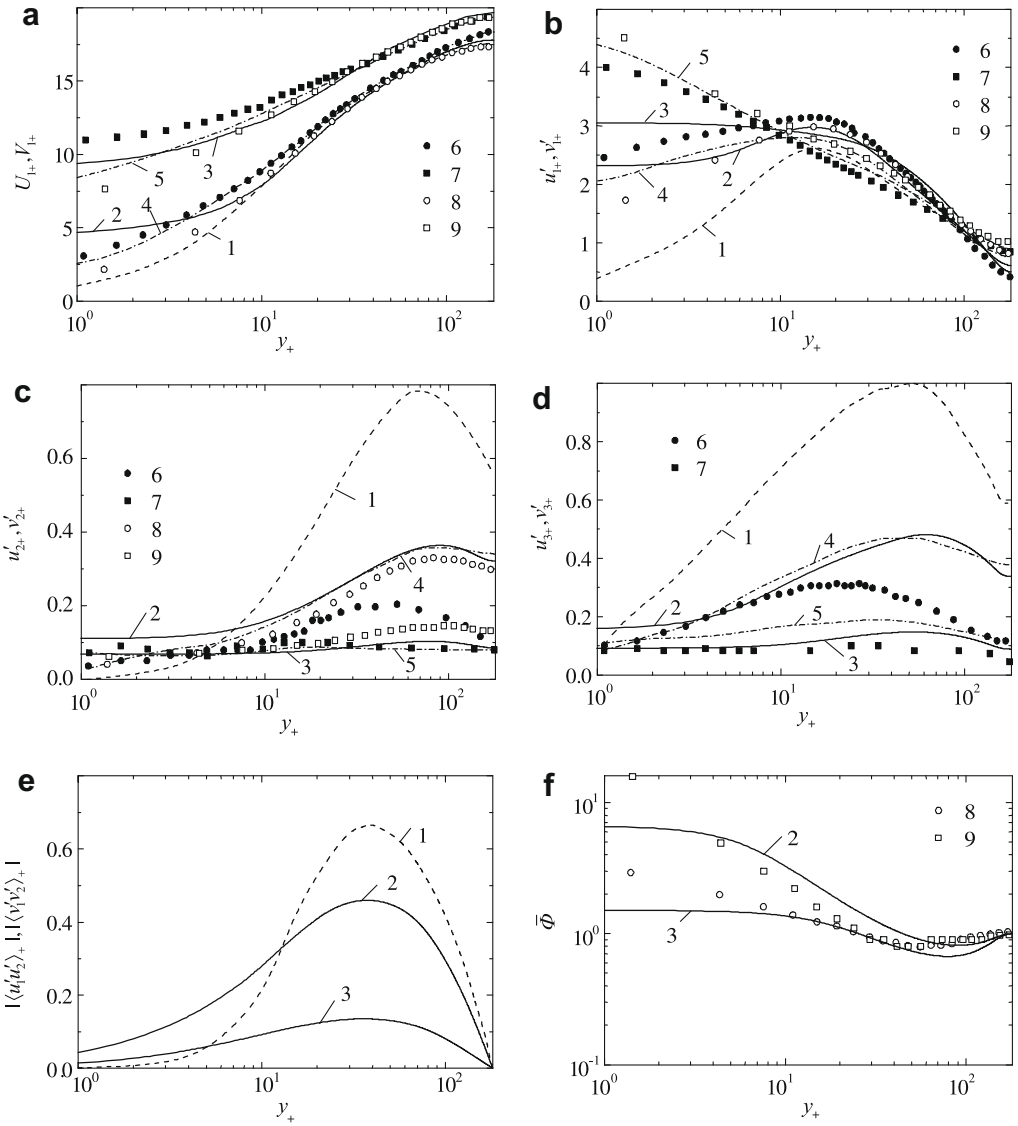

Fig. 2. Profiles of high-inertia particle characteristics over the channel cross-section: 1 – fluid; 2–9 – particles; 2, 3 – predictions; 4, 5 – LES by Wang and Squires (1996); 6, 7 – DNS by Rouson and Eaton (1994); 8, 9 – LES by Fukagata et al. (1998); 2, 4, 6, 8 – $\tau_+ = 117$; 3, 5, 7, 9 – $\tau_+ = 810$.

6. The effect of collisions on particle transport in a channel flow

Let us now examine the collision model presented in Section 3. Predictions are compared with LES by Vance et al. (2006) performed with and without inter-particle collisions in the absence of particle deposition and turbulence modulation by particles. In the simulations, particle–wall and particle–particle collisions were taken to be elastic. In this connection, all the restitution coefficients appearing in the collision terms and the boundary conditions were taken to be equal to unity. The bulk volume fraction, Φ_b, was fixed and equal to 2.3×10^{-4}.

Fig. 3 shows the effects of particle inertia and inter-particle collisions on the profiles of the average particle streamwise velocity, the wall-normal particle fluctuating velocity intensity, and the particle concentration. As is clear from the comparison of the results exhibited in Fig. 3a and 3b, the collisions exert a strong impact on the average particle streamwise velocity leading to its flattening and rising in the near-wall region. The reason is that the inter-particle collisions enhance the diffusion transport of particle velocity fluctuations in the normal direction. It should be point to a considerable discrepancy between the predictions and the simulations of V_{1+} with no collisions (Fig. 3a). According to Vance et al. (2006), the average streamwise velocity of high-inertia non-colliding particles is not too far removed from that of the fluid. We can not explain this discrepancy because the average streamwise velocities simulated by Vance et al. (2006) are in some contradiction with the numerical simulations presented in Fig. 2a, which suggested that V_{1+} was flattened with τ_+ for non-colliding particles. However, the predicted influence of collisions on V_{1+} is consistent with that simulated by Vance et al. (2006), although, as can be observed from Fig. 3b, the model predicts a somewhat less effect of collisions as compared with the simulated one for $\tau_+ = 468$.

It is clear from Fig. 3c that both the predictions and the simulations exhibit a decrease in the wall-normal velocity fluctuations with particle inertia when neglecting inter-particle collisions. This is due to the fact that high-inertia particles are less responsive to the velocity fluctuations of fluid turbulence. The behavior of wall-normal velocity fluctuations is crucial to explain a tendency of particles with a certain range of inertia to accumulate in the viscous sub-layer near the wall (Fig. 3e). Due to a gradient in the intensity of wall-normal velocity fluctuations, the particles tend to migrate to regions of lower turbulence en-

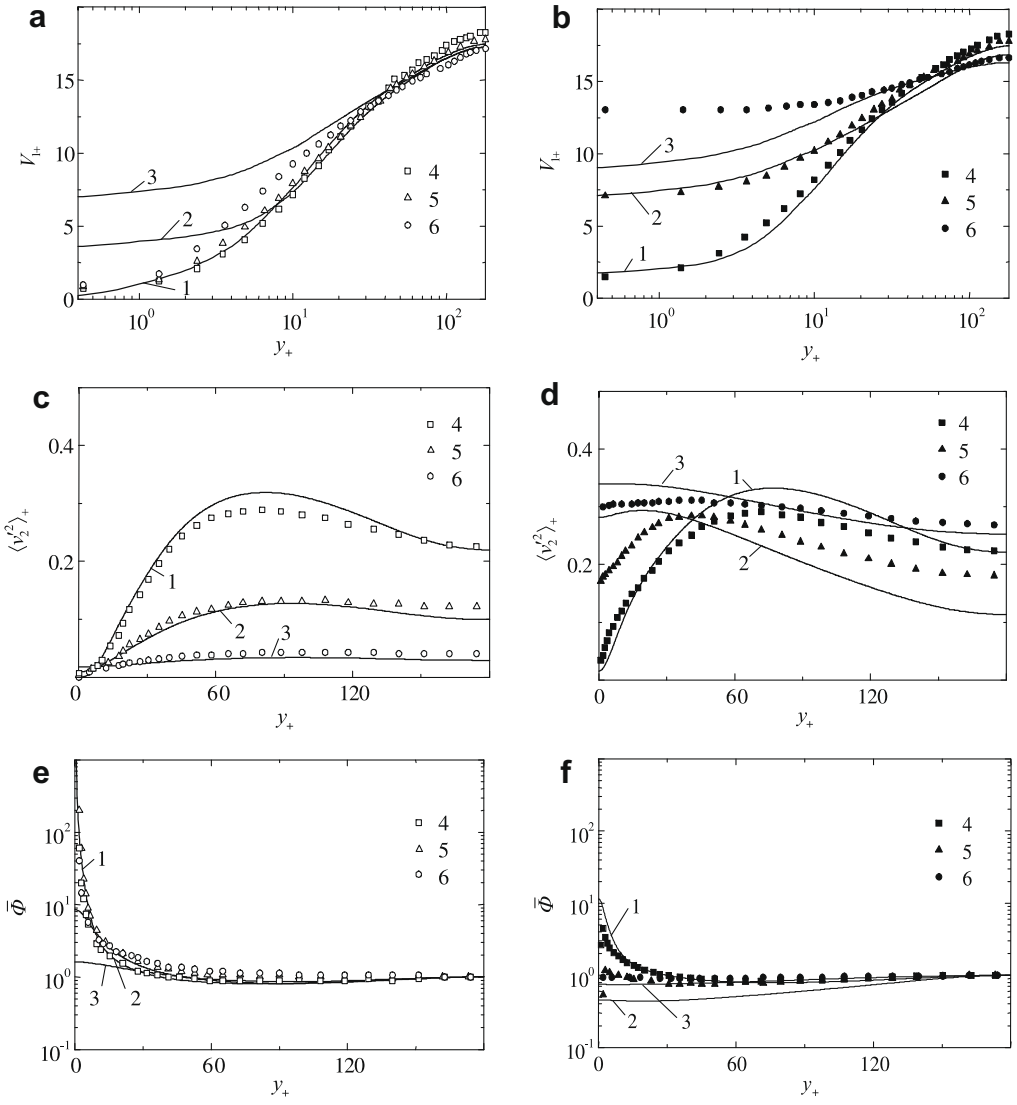

Fig. 3. Profiles of particle average streamwise velocity (a, b), wall-normal velocity fluctuations (c, d), and concentration (e, f): a, c, e – non-colliding particles; b, d, f – colliding particles; 1–3 – predictions; 4–6 – LES by Vance et al. (2006); 1, 4 – $\tau_+ = 29$; 2, 5 – $\tau_+ = 117$; 3, 6 – $\tau_+ = 468$.

ergy. In other words, the particles are pushed by the gradient of turbulence intensity towards the wall and "trapped" in the viscous wall region. Fig. 3d demonstrates a strong influence of collisions on the particle wall-normal velocity fluctuations. Owing to the mechanism of fluctuation redistribution from the streamwise velocity component, the wall-normal velocity fluctuations of colliding high-inertia particles can become quite large. Note that a decisive role of collisions in the generation of particle transverse velocity fluctuations was confirmed in experiments performed by Caraman et al. (2003) for particle-laden turbulent flow in a round tube.

Comparison of Fig. 3e and f shows the role of inter-particle collisions on the profile of particle concentration. The main conclusion drown from this comparison consists in reducing the accumulation of particles in the near-wall region as a result of collisions. In accordance with the LES of Vance et al. (2006), the model predicts that inter-particle collisions can lead even to a lesser concentration at the wall than at the channel axis. The levelling of particle distribution over the channel cross-section is attributable to intensification in the turbulent transport of particle velocity fluctuations due to collisions.

7. Deposition of particles from a channel flow

Finally let us consider the deposition of particles from a turbulent flow in a flat channel. Again, as in Sections 5 and 6, the flow is presumed to be fully developed. Therefore, all characteristics of the fluid and particulate phases, except for the particle fraction, can be treated as functions of the normal-wall coordinate y. The particle deposition rate, V_{2w}, is assumed to be constant, and hence the particle fraction falls exponentially with x_1. The rebound coefficient appearing in the boundary conditions (15) and (16) is taken as zero.

The most remarkable effect of particle deposition on the characteristics of the particulate phase over the channel cross-section consists in reducing the particle concentration in the near-wall region. As is seen from Fig. 4, in the absence of deposition, there is a monotonous increase in the concentration of not-too-high-inertia particles towards the wall, whereas a maximum of the particle concentration profile is observed in the viscous sub-layer when the deposition of such the particles takes place. Thus, the deposition results in decreasing the particle accumulation effect due to the removal of particles from the flow. The most pronounced accu-

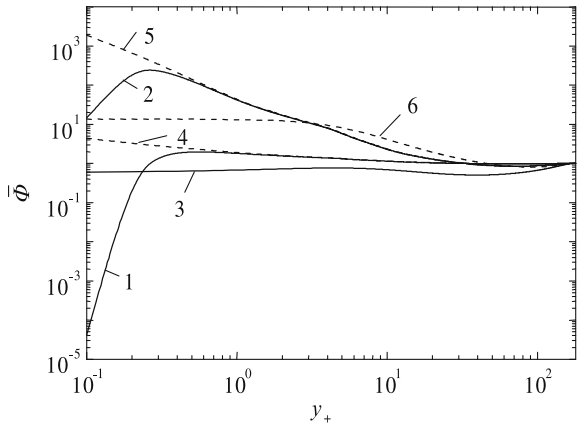

Fig. 4. Profiles of particle concentration: 1–3 – with deposition; 4–6 – without deposition; 1, 4 – $\tau_+ = 1$; 2, 5 – $\tau_+ = 10$; 3, 6 – $\tau_+ = 100$.

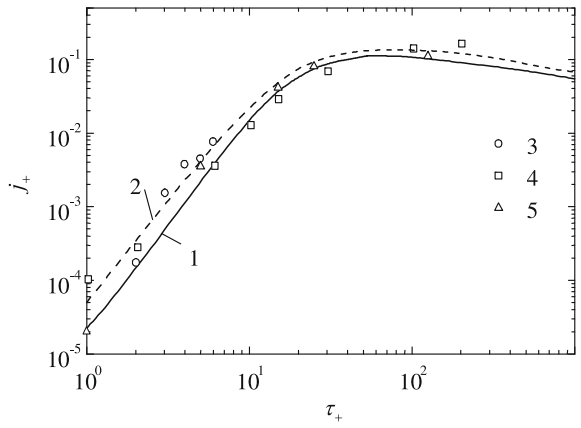

Fig. 5. The deposition coefficient versus the particle inertia parameter: 1 and 2 – predictions for non-colliding and colliding particles, 3 – DNS by McLaughlin (1989), 4 – LES by Wang et al. (1997), 5 – DNS by Marchioli et al. (2007).

mulation of deposing particles is predicted for $\tau_+ \approx 10$, which is in good agreement with the value of τ_+ obtained in numerical simulations by Chen and McLaughlin (1995) when the maximum of the particle concentration profile was achieved.

Fig. 5 shows the deposition coefficient, which is the particle deposition flow rate normalized with the friction velocity and the bulk particle fraction, as a function of the particle inertia parameter. Predictions with no collisions (curve 1) are compared with numerical simulations by McLaughlin (1989), Wang et al. (1997), and Marchioli et al. (2007). As is clear, there are two distinctive regions, in which an increase or a decrease in j_+ with τ_+ takes place. The increase in j_+ with τ_+ is due to the turbophoresis effect induced by the gradient in velocity fluctuations, and the decrease in j_+ with τ_+ is caused by a low response of high-inertia particles to the fluid turbulence. In Fig. 5, the dependence of j_+ on τ_+ is also depicted when allowing for elastic inter-particle collisions for $\Phi_b = 10^{-4}$ (curve 2). The influence of collisions leads to an augmentation of the deposition process, which is in accordance with DNS performed recently by Nasr et al. (2007). This enhancement of j_+ is caused by the increase in the wall-normal fluctuating velocity, which is mainly responsible for the deposition of particle in turbulent vertical channel flow, due to the redistribution mechanism induced by collisions.

8. Summary

A statistical approach for predicting the transport and deposition of inertial colliding particles in turbulent flows is advanced. The approach is based on a kinetic equation for the PDF of particle velocity distribution. This kinetic equation allows for the particle–turbulence and particle–particle interactions. The kinetic PDF equation generates a set of governing equations for the transport of the particulate phase. The collision terms appearing in governing equations are obtained using a Grad-like expansion of the two-particle velocity PDF.

The validity of the models presented is established by means of comparisons with numerical simulations performed in vertical flat channel flows with and without both inter-particle collisions and particle deposition onto the channel wall. On the basis of comparisons with numerical simulations, it can be concluded that the models are able to capture the main features of transport, deposition, and preferential concentration of non-colliding and colliding particles in turbulent channel flows.

The main predicted effects of collisions on the particulate phase consist in flattening the average streamwise velocity, increasing the transverse fluctuating velocity, and decreasing the preferential accumulation in the near-wall region of the flow as well al in enhancing the deposition rate.

Acknowledgment

This work was supported by the Russian Foundation for Basic Research (Grant Numbers 07-08-92160 and 08-08-12229).

Appendix Particle–turbulence interaction

Using the Furutsu–Donsker–Novikov formula for Gaussian random functions and applying an iteration procedure, we can derive (Zaichik, 1999; Zaichik et al., 2004; Zaichik and Alipchenkov, 2005)

$$\lambda_{ij} = \langle u_i' u_k' \rangle \left(\frac{f_{u\,kj}}{\tau_p} + l_{u\,kn} \frac{\partial U_j}{\partial x_n} + \tau_p m_{u\,kl} \frac{\partial U_n}{\partial x_l} \frac{\partial U_j}{\partial x_n} \right) - \frac{1}{2} \frac{D_p \langle u_i' u_k' \rangle}{Dt} \left(f_{u1\,kj} + \tau_p l_{u1\,kn} \frac{\partial U_j}{\partial x_n} \right),$$

$$\mu_{ij} = \langle u_i' u_k' \rangle \left(g_{u\,kj} + \tau_p h_{u\,kn} \frac{\partial U_j}{\partial x_n} \right) - \frac{\tau_p}{2} \frac{D_p \langle u_i' u_k' \rangle}{Dt} g_{u1\,kj},$$

$$\frac{D_p \langle u_i' u_j' \rangle}{Dt} = \frac{\partial \langle u_i' u_j' \rangle}{\partial t} + U_{p\,k} \frac{\partial \langle u_i' u_j' \rangle}{\partial x_k} + \frac{\partial \langle u_i' u_j' u_k' \rangle_p}{\partial x_k},$$

$$U_{p\,i} = U_i - \tau_p \mu_{ij} \frac{\partial \ln \Phi}{\partial x_j},$$

$$\langle u_i' u_j' u_k' \rangle_p = -\frac{\tau_p}{3} \left(\mu_{in} \frac{\partial \langle u_j' u_k' \rangle}{\partial x_n} + \mu_{jn} \frac{\partial \langle u_i' u_k' \rangle}{\partial x_n} + \mu_{kn} \frac{\partial \langle u_i' u_j' \rangle}{\partial x_n} \right),$$

where $f_{u\,ij}$, $g_{u\,ij}$, $l_{u\,ij}$, $h_{u\,ij}$, $m_{u\,ij}$, $f_{u1\,ij}$, $g_{u1\,ij}$, and $l_{u1\,ij}$ are the tensor coefficients that measure a response of particles to the fluid turbulence, i.e., a coupling between the fluid and particulate phases. These are functions of the particle response time, τ_p, related to the Lagrangian timescales of the fluid velocity seen by the particles (the so-called eddy–particle interaction timescales), $T_{Lp\,ij}$. For the purpose of further simplification, the Lagrangian timescale tensor of fluid turbulence, $T_{L\,ij}$, is assumed to be isotropic, $T_{L\,ij} = T_L \delta_{ij}$. And yet we shall still take into account the different timescales of particle interaction with turbulent eddies in different directions – a phenomenon that arises as a consequence of the "crossing-trajectories effect" (Csanady, 1963). As a result, we shall still observe the distinction between the longitudinal (in x_1-direction), T_{Lp}^l, and transverse (in x_2- and x_3-directions), T_{Lp}^n, components of $T_{Lp\,ij}$. In order to determine the response coefficients, it is necessary to specify the autocorrelation function of the fluid velocity seen by inertial particles. When using

the two-scale bi-exponential autocorrelation function like that proposed by Sawford (1991), the response coefficients to be needed take the form

$$f_u^\varsigma = \frac{2\Omega_\varsigma + z_\varsigma^2}{2\Omega_\varsigma + 2\Omega_\varsigma^2 + z_\varsigma^2}, \quad g_u^\varsigma = \frac{1}{\Omega_\varsigma} - f_u^\varsigma, \quad l_u^\varsigma = g_u^\varsigma - f_{u1}^\varsigma$$

$$h_u^\varsigma = \frac{2 - 4\Omega_\varsigma - z_\varsigma^2}{2\Omega_\varsigma^2} + 2f_u^\varsigma + f_{u1}^\varsigma, \quad f_{u1}^\varsigma = \frac{(2\Omega_\varsigma + z_\varsigma^2)^2 - 2\Omega_\varsigma^2 z_\varsigma^2}{(2\Omega_\varsigma + 2\Omega_\varsigma^2 + z_\varsigma^2)^2},$$

$$g_{u1}^\varsigma = \frac{2 - z_\varsigma^2}{2\Omega_\varsigma^2} - f_{u1}^\varsigma, \quad l_{u1}^\varsigma = g_{u1}^\varsigma - \frac{2[(2\Omega_\varsigma + z_\varsigma^2)^3 - 6\Omega_\varsigma^2 z_\varsigma^4 - 8\Omega_\varsigma^3 z_\varsigma^2]}{(2\Omega_\varsigma + 2\Omega_\varsigma^2 + z_\varsigma^2)^3},$$

$$\Omega_\varsigma = \frac{\tau_p}{T_{Lp}^\varsigma}, \quad z_\varsigma = \frac{\tau_T}{T_{Lp}^\varsigma}, \qquad \varsigma - l, n.$$

Here τ_T is the Taylor differential timescale of fluid turbulence that is determined as (Zaichik et al., 2003)

$$\tau_T = \left(\frac{2Re_\lambda}{15^{1/2} a_0}\right)^{1/2} \tau_k, \qquad a_0 = \frac{a_{01} + a_{0\infty} Re_\lambda}{a_{02} + Re_\lambda}, \quad a_{01} = 11,$$

$$a_{02} = 205, \quad a_{0\infty} = 7.$$

The eddy–particle interaction timescales are determined using the model presented by Oesterlé and Zaichik (2006)

$$T_{Lp}^l = \left\{\frac{3\Im + m(2+3\gamma^2)}{3\Im(1+m\Im)^2} + \left[\frac{1}{1+m\gamma} - \frac{3\Im + m(2+3\gamma^2)}{3\Im(1+m\Im)^2}\right] f(St_E)\right\} T_E,$$

$$T_{Lp}^n = \left\{\frac{6\Im + m(4+3\gamma^2)}{6\Im(1+m\Im)^2} + \left[\frac{2+m\gamma}{2(1+m\gamma)^2} - \frac{6\Im + m(4+3\gamma^2)}{6\Im(1+m\Im)^2}\right] f(St_E)\right\} T_E,$$

$$T_E = \frac{3(1+m)^2}{3+2m} T_L, \quad \gamma = \frac{|V_1 - U_1|}{(2k/3)^{1/2}}, \quad \Im = (1+\gamma^2)^{1/2},$$

$$f(St_E) = \frac{St_E}{1+St_E} - \frac{0.9 m St_E^2}{(1+St_E)^2(2+St_E)}.$$

For the flows under consideration, the turbulence structure parameter is taken as $m = 0.5$ and the Lagrangian integral timescale is given by

$$T_L = \left[\left(\frac{\alpha_1 \nu}{u_*^2}\right)^2 + \left(\frac{\alpha_2 k}{\varepsilon}\right)^2\right]^{1/2}, \qquad \alpha_1 = 10, \quad \alpha_2 = 0.3.$$

The response coefficient that appears in the collision terms is determined as

$$f_u = \frac{f_u^l + 2f_u^n}{3}.$$

References

Alipchenkov, V.M., Zaichik, L.I., Simonin, O., 2001. A comparison of two approaches to derivation of boundary conditions for continuous equations of particle motion in turbulent flow. High Temp. 39, 104–110.

Caporaloni, M., Tampieri, F., Trombetti, F., Vittori, O., 1975. Transfer of particles in nonisotropic air turbulence. J. Atmos. Sci. 32, 565–568.

Caraman, N., Borée, J., Simonin, O., 2003. Effect of collisions on the dispersed phase fluctuation in a dilute tube flow: experimental and theoretical analysis. Phys. Fluids 15, 3602–3612.

Chen, M., McLaughlin, J.B., 1995. A new correlation for the aerosol deposition rate in vertical ducts. J. Colloid Interface Sci. 169, 437–455.

Csanady, G.T., 1963. Turbulent diffusion of heavy-particles in the atmosphere. J. Atmos. Sci. 20, 201–208.

Fukagata, K., Zahrai, S., Bark, F.H., 1998. Force balance in a turbulent particulate channel flow. Int. J. Multiphase Flow 24, 867–887.

Jenkins, J.T., Richman, M.W., 1985. Grad's 13-moment system for a dense gas of inelastic spheres. Arch. Ration. Mech. Anal. 87, 355–377.

Laviéville, J., Deutsch, E., Simonin, O., 1995. Large eddy simulation of interactions between colliding particles and a homogeneous isotropic turbulence field. In: Proceedings of the Sixth International Symposium on Gas–Solid Flows. ASME FED 228. pp. 347–357.

Laviéville, J., Simonin, O., Berlemont, A., Chang, Z., 1997. Validation of inter-particle collision models based on large eddy simulation in gas–solid turbulent homogeneous shear flow. In: Proceedings of the Seventh International Symposium on Gas-particle Flows. ASME Fluids Engineering Division Summer Meeting. FEDSM97-3623.

Lee, S.L., Durst, F., 1982. On the motion of particles in turbulent duct flows. Int. J. Multiphase Flow 8, 125–146.

Marchioli, C., Soldati, A., 2002. Mechanisms for particle transport and segregation in a turbulent boundary layer. J. Fluid Mech. 468, 283–315.

Marchioli, C., Picciotto, M., Soldati, A., 2007. Influence of gravity and lift on particle velocity statistics and transfer rates in turbulent vertical channel flow. Int. J. Multiphase Flow 33, 227–251.

McLaughlin, J., 1989. Aerosol particle deposition in numerically simulated channel flow. Phys. Fluids A 1, 1211–1224.

Nasr, H., Ahmadi, G., McLaughlin, J., 2007. Effects of inter-particle collisions and two-way coupling on particle deposition velocity in a turbulent channel flow. In: Proceedings of the Sixth International Conference on Multiphase Flow. Leipzig, Germany.

Oesterlé, B., Zaichik, L.I., 2006. Time scales for predicting dispersion of arbitrary-density particles in isotropic turbulence. Int. J. Multiphase Flow 32, 838–849.

Picciotto, M., Marchioli, C., Reeks, M.W., Soldati, A., 2005. Statistics of velocity and preferential concentration of micro-particles in boundary layer turbulence. Nucl. Eng. Des. 235, 1239–1249.

Reeks, M.W., 1983. The transport of discrete particles in inhomogeneous turbulence. J. Aerosol Sci. 14, 729–739.

Rotta, J.C., 1951. Statistische Theorie nichthomogener Turbulenz. Z. Phys. 129, 547–572.

Rouson, D.W.I., Eaton, J.K., 1994. Direct numerical simulation of particles interacting with a turbulent channel flow. In: Proceedings of the Seventh Workshop on Two-phase Flow Predictions. Erlangen, Germany.

Sawford, B.L., 1991. Reynolds number effects in Lagrangian stochastic models of turbulent dispersion. Phys. Fluids A 3, 1577–1586.

Simonin, O., 1991. Second-moment prediction of dispersed-phase turbulence in particle-laden flows. In: Proceedings of the Eighth Symposium on Turbulent Shear Flows. Munich, Germany, pp. 741–746.

Simonin, O., 1996. Combustion and Turbulence in Two-phase Flows: Continuum Modelling of Dispersed Two-phase Flows. Lecture Series 1996-02. Von Karman Institute for Fluid Dynamics, Belgium.

Tsuji, Y., Morikawa, Y., Shiomi, H., 1984. LDV measurements of an air–solid two-phase flow in a vertical pipe. J. Fluid Mech. 139, 417–434.

Vance, M.W., Squires, K.D., Simonin, O., 2006. Properties of the particle velocity field in gas–solid turbulent channel flow. Phys. Fluids 18, 063302-1–063302-13.

Wang, Q., Squires, K.D., 1996. Large eddy simulation of particle-laden turbulent channel flow. Phys. Fluids 8, 1207–1223.

Wang, Q., Squires, K.D., Chen, M., McLaughlin, J.B., 1997. On the role of the lift force in turbulence simulations of particle deposition. Int. J. Multiphase Flow 23, 749–763.

Zaichik, L.I., 1999. A statistical model of particle transport and heat transfer in turbulent shear flows. Phys. Fluids 11, 1521–1534.

Zaichik, L.I., Alipchenkov, V.M., 2001. A statistical model for transport and deposition of high-inertial colliding particles in turbulent flow. Int. J. Heat Fluid Flow 22, 365–371.

Zaichik, L.I., Alipchenkov, V.M., 2005. Statistical models for predicting particle dispersion and preferential concentration in turbulent flows. Int. J. Heat Fluid Flow 26, 416–430.

Zaichik, L.I., Simonin, O., Alipchenkov, V.M., 2003. Two statistical models for predicting collision rates of inertial particles in homogeneous isotropic turbulence. Phys. Fluids 15, 2995–3005.

Zaichik, L.I., Oestterlé, B., Alipchenkov, V.M., 2004. On the probability density function model for the transport of particles in anisotropic turbulent flow. Phys. Fluids 16, 1956–1964.